Duocarmycin SA Shortened, Simplified, and Extended Agents: A Systematic Examination of the Role of the DNA Binding Subunit

Dale L. Boger,* Donald L. Hertzog, Bernd Bollinger, Douglas S. Johnson, Hui Cai, Joel Goldberg, and Philip Turnbull

Contribution from the Department of Chemistry, The Scripps Research Institute, 10550 North Torrey Pines Road, La Jolla, California 92037

Received October 25, 1996[⊗]

Abstract: The examination of shortened, simplified, and extended analogs of duocarmycin SA is described and constitutes a detailed study of the role of linked DNA binding subunit. In addition to enhancing the DNA binding affinity and selectivity through minor groove noncovalent contacts, the studies in conjunction with those of the accompanying article illustrate that an extended rigid N^2 amide substituent is required for catalysis of the DNA alkylation reaction. This activation for DNA alkylation is independent of pH, and we propose it results from a binding-induced conformational change in the agents which increases their inherent reactivity. The ground state destabilization of the substrate results from a twist in the linking amide that disrupts the vinylogous amide stabilization of the alkylation subunit and activates the agent for nucleophilic addition. This leads to preferential activation of the agents for DNA alkylation within the narrower, deeper AT-rich minor groove sites where the inherent twist in the linking amide and helical rise of the bound conformation is greatest. Thus, shape-selective recognition (preferential AT-rich noncovalent binding) and shape-dependent catalysis (induced twist in linking N^2 amide) combine to restrict S_N2 alkylation to accessible adenine N3 nucleophilic sites within the preferred binding sites. Additional ramifications of this DNA binding-induced conformational change on the reversibility of the DNA alkylation reaction are discussed. The results of the study illustrate the importance of the C5′ methoxy group and the C6 methyl ester of duocarmycin SA, and a previously unrecognized role for these substituents is proposed.

Duocarmycin SA (**1**)[1] and duocarmycin A (**2**)[2] constitute the parent members of a class of potent antitumor antibiotics[3] related to CC-1065 (**3**)[4] that derive their properties through a sequence-selective alkylation of duplex DNA (Figure 1).[5−12] Since their disclosure, substantial efforts have been devoted to defining the characteristics of their DNA alkylation reactions, to determining the origin of their DNA alkylation selectivity, and to defining fundamental relationships between structure, functional reactivity, and biological properties.[5,6]

Herein, we report the synthesis and evaluation of shortened, simplified, and extended analogs of duocarmycin SA constituting a detailed examination of the DNA binding subunit of the natural product.[13−15] In the accompanying paper,[16] we report the complementary examination of reversed and sandwiched analogs of duocarmycin SA. In addition to their inherent importance as analogs of duocarmycin SA, the side-by-side

[⊗] Abstract published in *Advance ACS Abstracts,* May 1, 1997.

(1) Ichimura, M.; Ogawa, T.; Takahashi, K.; Kobayashi, E.; Kawamoto, I.; Yasuzawa, T.; Takahashi, I.; Nakano, H. *J. Antibiot.* **1990**, *43*, 1037.

(2) Takahashi, I.; Takahashi, K.; Ichimura, M.; Morimoto, M.; Asano, K.; Kawamoto, I.; Tomita, F.; Nakano, H. *J. Antibiot.* **1988**, *41*, 1915.

(3) Yasuzawa, T.; Muroi, K.; Ichimura, M.; Takahashi, I.; Ogawa, T.; Takahashi, K.; Sano, H.; Saitoh, Y. *Chem. Pharm. Bull.* **1995**, *43*, 378.

(4) Chidester, C. G.; Krueger, W. C.; Mizsak, S. A.; Duchamp, D. J.; Martin, D. G. *J. Am. Chem. Soc.* **1981**, *103*, 7629.

(5) Hurley, L. H.; Needham-VanDevanter, D. R. *Acc. Chem. Res.* **1986**, *19*, 230. Warpehoski, M. A.; Hurley, L. H. *Chem. Res. Toxicol.* **1988**, *1*, 315. Warpehoski, M. A. In *Advances in DNA Sequence Specific Agents*; Hurley, L. H., Ed.; JAI: Greenwich, CT, 1992; Vol. 1, p 217. Hurley, L. H.; Draves, P. H. In *Molecular Aspects of Anticancer Drug-DNA Interactions*; Neidle, S., Waring, M., Eds.; CRC: Ann Arbor, MI, 1993; Vol. 1, p 89. Aristoff, P. A. In *Advances in Medicinal Chemistry*; JAI: Greenwich, CT, 1993; Vol. 2, p 67.

(6) Boger, D. L.; Johnson, D. S. *Angew Chem., Int. Ed. Engl.* **1996**, *35*, 1439. Boger, D. L.; Johnson, D. S. *Proc. Natl. Acad. Sci. U.S.A.* **1995**, *92*, 3642. Boger, D. L. *Acc. Chem. Res.* **1995**, *28*, 20. Boger, D. L. In *Advances in Heterocyclic Natural Product Synthesis*; Pearson, W. H., Ed.; JAI: Greenwich, CT, 1992; Vol. 2, p 1. Boger, D. L. *Chemtracts: Org. Chem.* **1991**, *4*, 329. Boger, D. L. In *Proc. R. A. Welch Found. Conf. Chem. Res., XXXV., Chem. Frontiers Med.* **1991**, *35*, 137. Boger, D. L. In *Heterocycles in Bioorganic Chemistry*; Bergman, J., van der Plas, H. C., Simonyl, M., Eds.; Royal Society of Chemistry: Cambridge, 1991; p 103. Coleman, R. S.; Boger, D. L. In *Studies in Natural Products Chemistry*; Rahman, A.u., Ed.; Elsevier: Amsterdam, The Netherlands, 1989; Vol. 3, p 301.

(7) Boger, D. L.; Johnson, D. S.; Yun, W. *J. Am. Chem. Soc.* **1994**, *116*, 1635.

(8) Boger, D. L.; Yun, W. *J. Am. Chem. Soc.* **1993**, *115*, 9872.

(9) Boger, D. L.; Ishizaki, T.; Zarrinmayeh, H.; Munk, S. A.; Kitos, P. A.; Suntornwat, O. *J. Am. Chem. Soc.* **1990**, *112*, 8961. Boger, D. L.; Ishizaki, T.; Zarrinmayeh, H.; Kitos, P. A.; Suntornwat, O. *J. Org. Chem.* **1990**, *55*, 4499. Boger, D. L.; Ishizaki, T.; Zarrinmayeh, H. *J. Am. Chem. Soc.* **1991**, *113*, 6645. Boger, D. L.; Yun, W.; Terashima, S.; Fukuda, Y.; Nakatani, K.; Kitos, P. A.; Jin, Q. *Bioorg. Med. Chem. Lett.* **1992**, *2*, 759.

(10) Boger, D. L.; Johnson, D. S.; Yun, W.; Tarby, C. M. *Bioorg. Med. Chem.* **1994**, *2*, 115. Boger, D. L.; Munk, S. A.; Zarrinmayeh, H.; Ishizaki, T.; Haught, J.; Bina, M. *Tetrahedron* **1991**, *47*, 2661. Boger, D. L.; Coleman, R. S.; Invergo, B. J.; Sakya, S. M.; Ishizaki, T.; Munk, S. A.; Zarrinmayeh, H.; Kitos, P. A.; Thompson, S. C. *J. Am. Chem. Soc.* **1990**, *112*, 4623.

(11) Sugiyama, H.; Hosada, M.; Saito, I.; Asai, A.; Saito, H. *Tetrahedron Lett.* **1990**, *31*, 7197. Sugiyama, H.; Ohmori, K.; Chan, K. L.; Hosoda, M.; Asai, A.; Saito, H.; Saito, I. *Tetrahedron Lett.* **1993**, *34*, 2179. Yamamoto, K.; Sugiyama, H.; Kawanishi, S. *Biochemistry* **1993**, *32*, 1059. Asai, A.; Nagamura, S.; Saito, H. *J. Am. Chem. Soc.* **1994**, *116*, 4171.

(12) Reynolds, V. L.; Molineux, I. J.; Kaplan, D. J.; Swenson, D. H.; Hurley, L. H. *Biochemistry* **1985**, *24*, 6228. Hurley, L. H.; Lee, C.-S.; McGovren, J. P.; Warpehoski, M. A.; Mitchell, M. A.; Kelly, R. C.; Aristoff, P. A. *Biochemistry* **1988**, *27*, 3886. Hurley, L. H.; Warpehoski, M. A.; Lee, C.-S.; McGovren, J. P.; Scahill, T. A.; Kelly, R. C.; Mitchell, M. A.; Wicnienski, N. A.; Gebhard, I.; Johnson, P. D.; Bradford, V. S. *J. Am. Chem. Soc.* **1990**, *112*, 4633.

(13) Boger, D. L.; Bollinger, B.; Johnson, D. S. *Bioorg. Med. Chem. Lett.* **1996**, *6*, 2207.

(14) Boger, D. L.; Goldberg, J.; McKie, J. A. *Bioorg. Med. Chem. Lett.* **1996**, *6*, 1955.

(15) Boger, D. L.; Garbaccio, R. M. *Bioorg. Med. Chem.* **1997**, *5*, 263.

(16) Boger, D. L.; Bollinger, B.; Hertzog, D. L.; Johnson, D. S.; Cai, H.; Mésini, P.; Garbaccio, R. M.; Jin, Q.; Kitos, P. A. *J. Am. Chem. Soc.* **1997**, *119*, 4987−4998.

S0002-7863(96)03720-1 CCC: $14.00

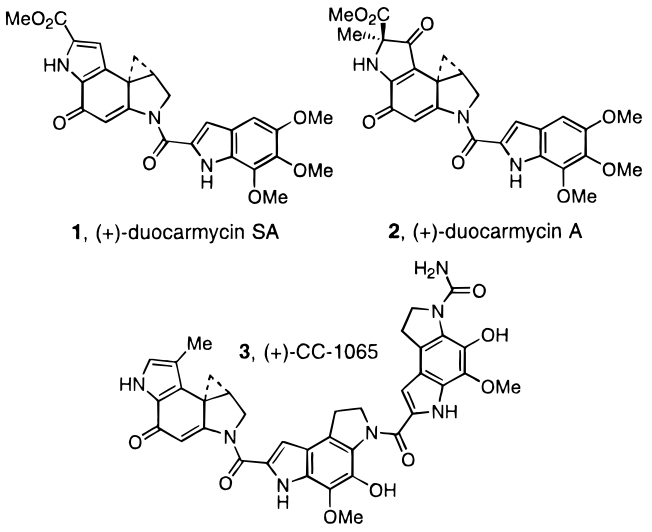

Figure 1.

Scheme 1

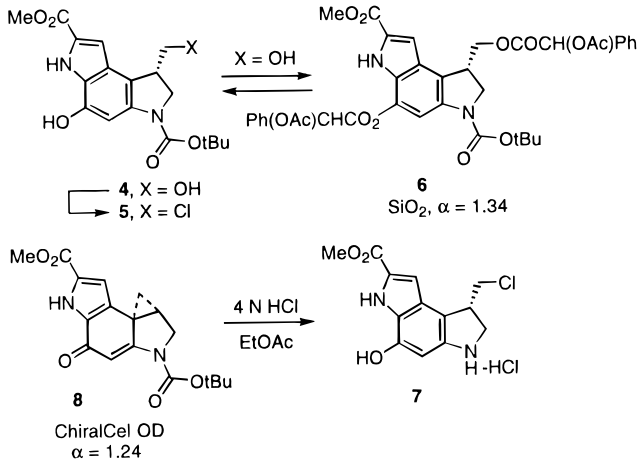

comparisons of the three classes of agents have provided an unambiguous demonstration of the basis for the sequence-selective alkylation of duplex DNA and have defined previously unrecognized structural features that contribute to the catalysis of the reaction.

Synthesis

Resolution of *N*-BOC-DSA. The optically active agents were prepared through chromatographic resolution of the bis-(*R*)-*O*-acetylmandelate ester of **6**[17] or, more conveniently, through a new protocol of direct chromatographic resolution of *N*-BOC-DSA (**8**). Although the immediate precursors to **8**, including **4** and **5**, were not resolved by direct chromatographic means, the enantiomers of *N*-BOC-DSA were effectively separated on a semipreparative ChiralCel OD HPLC column (10 μm 2 × 25 cm, 30% 2-propanol/hexane, 7 mL/min, α = 1.24, ≥99.9% enantiomeric excess (ee)). Acid-catalyzed deprotection of **8** (4 N HCl/EtOAc, 25 °C, 30 min, 95−100%) was accompanied by clean addition of HCl to the cyclopropane and provided **7** (Scheme 1). Notably, no trace of the ring expansion product derived from addition of chloride to the more substituted C8a cyclopropane carbon was detected.

Simple Derivatives of the Alkylation Subunit. In studies that culminated in the total synthesis of (+)- and *ent*-(−)-**1**, we detailed the synthesis and examination of both enantiomers of

Scheme 2

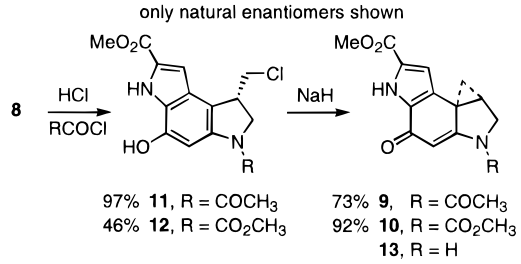

Scheme 3

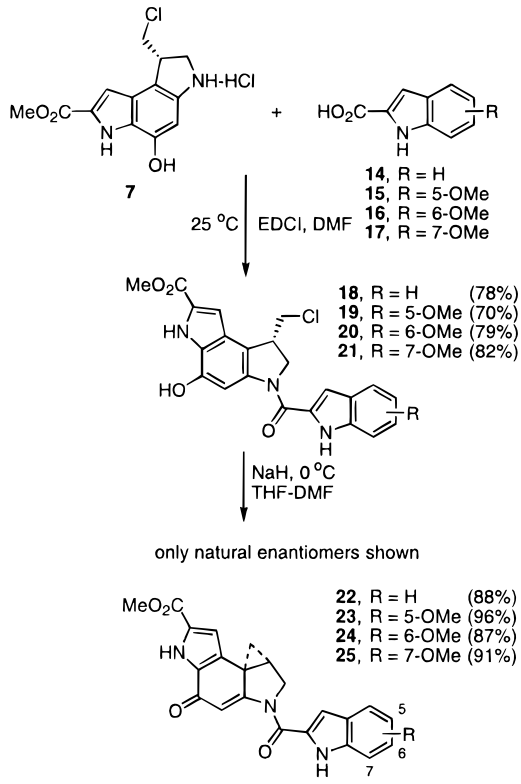

N-BOC-DSA (**8**) and DSA (**13**).[7,17] To generalize the properties of such simple derivatives, both enantiomers of **9** and **10** were prepared (Scheme 2). Treatment of **8** with 4 N HCl/EtOAc (25 °C, 30 min) followed by acylation with acetyl chloride or methyl chloroformate (2.0 equiv, 3.0 equiv of $NaHCO_3$, THF, 25 °C, 1 h) provided **11** (97%) and **12** (46%). Spirocyclization to provide **9** (73%) and **10** (92%) was effected by treatment with NaH.

Modifications in the Right-Hand Subunit: Role of the Methoxy Substituents. We elected to examine modifications in the trimethoxyindole subunit of duocarmycin SA with the intention of defining the role of each of the three methoxy substituents.[13] Treatment of **8** with 4 N HCl/EtOAc (25 °C, 30 min) followed by coupling (3 equiv of EDCI, DMF, 25 °C, 4−15 h) of **7** with **14**−**17** (1.1 equiv) in the absence of added base[18] provided the precursors **18**−**21** (70−82%, Scheme 3). Spirocyclization was effected by treatment with NaH (3 equiv, THF/DMF 4−2:1, 0 °C, 30 min) to provide of **22**−**25** (87−96%). Coupling of **7** in the presence of a base such as $NaHCO_3$ led to competitive spirocyclization, and the presence of adventitious moisture in the spirocyclization reaction mixture led to subsequent hydrolysis of the linking N^2 amide.

Substitutions for the DNA Binding Subunit: Extended Analogs. In preceding studies, three additional DNA binding

(17) Boger, D. L.; Machiya, K.; Hertzog, D. L.; Kitos, P. A.; Holmes, D. *J. Am. Chem. Soc.* **1993**, *115*, 9025.

(18) Boger, D. L.; Ishizaki, T.; Kitos, P. A.; Suntornwat, O. *J. Org. Chem.* **1990**, *55*, 5823.

Scheme 4

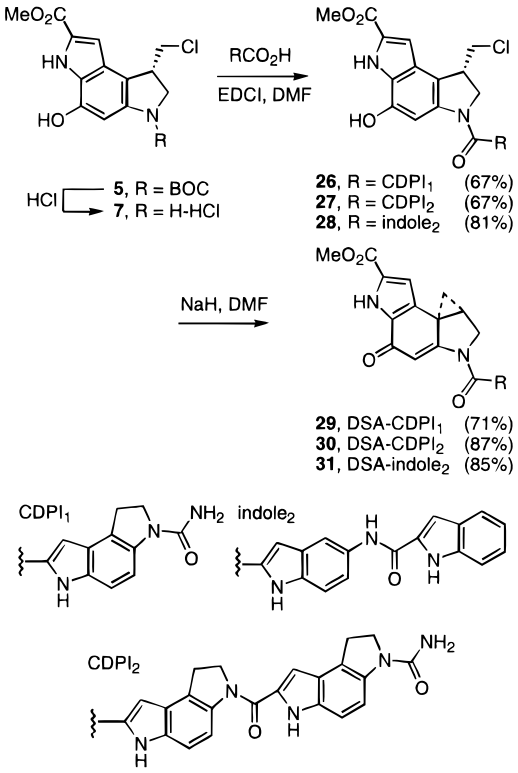

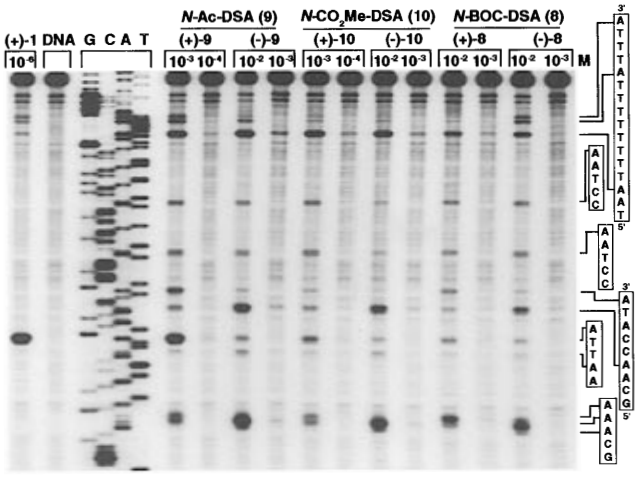

Figure 2. Thermally-induced strand cleavage of w794 DNA (144 bp, nucleotide no. 5238−138) after DNA−agent incubation at 37 °C for 24 h, removal of unbound agents by EtOH precipitation, and 30 min of thermolysis (100 °C), followed by denaturing 8% PAGE and autoradiography. Lane 1, (+)-duocarmycin SA (1×10^{-6} M); lane 2, control DNA; lanes 3−6, Sanger G, C, A, and T sequencing standards; lanes 7 and 8, (+)-*N*-Ac-DSA (**9**, 1×10^{-3} to 1×10^{-4} M); lanes 9 and 10, (−)-*N*-Ac-DSA (**9**, 1×10^{-2} to 1×10^{-3} M); lanes 11 and 12, (+)-*N*-CO_2Me-DSA (**10**, 1×10^{-3} to 1×10^{-4} M); lanes 13 and 14, (−)-*N*-CO_2Me-DSA (**10**, 1×10^{-2} to 1×10^{-3} M); lanes 15 and 16, (+)-*N*-BOC-DSA (**8**, 1×10^{-2} to 1×10^{-3} M); lanes 17 and 18, (−)-*N*-BOC-DSA (**8**, 1×10^{-2} to 1×10^{-3} M).

subunits have proven to be representative and important to examine[5−10] and these are $CDPI_1$,[19] $CDPI_2$,[19] and $indole_2$. The former typically provides agents analogous to **1** and **2** while the latter two derivatives are representative of the larger agents which exhibit a more extended 5 base-pair (bp) AT-rich DNA alkylation selectivity analogous to CC-1065 (**3**). In addition, the $indole_2$ derivatives maintain the cytotoxic potency of **1**−**3**, but typically exhibit more efficacious in vivo antitumor activity.[20] The agents were prepared by acid-catalyzed deprotection of **5** (4 N HCl/EtOAc, 25 °C, 15−20 min) followed by immediate coupling (3 equiv of EDCI, DMF, 12−24 h, 25 °C) of **7** with $CDPI_1$[19] (67%), $CDPI_2$[19] (67%), and $indole_2$ (81%) conducted in the absence of added base (Scheme 4). Spirocyclization to provide **29**−**31** was effected by treatment with NaH.

Properties

DNA Alkylation Efficiency and Selectivity. The DNA alkylation properties of the agents were examined within five 145−155 base-pair segments of DNA. The five clones of phage M13mp10 contain SV40 nucleosomal DNA inserts: w794 (nucleotide no. 5238−138) and its complement w836 (nucleotide no. 5189−91), c988 (nucleotide no. 4359−4210) and its complement c820 (nucleotide no. 4196−4345), and c1346 (nucleotide no. 1632−1782).[10] The alkylation site identification and the assessment of the relative selectivity among the available sites were obtained by thermally-induced strand cleavage of the singly 5′ end-labeled duplex DNA after exposure to the agents as previously detailed.[10] A statistical treatment of the alkylation sites proved more revealing than a conventional analysis that considers only the observed alkylation sites. This evaluation, which includes the consideration of sites *not* alkylated, helped to define the composite consensus sequence and highlighted subtle features not apparent from a simple consideration only of the alkylated sites.

Simple Derivatives of the Alkylation Subunit. A representative comparison of both enantiomers of **9** and **10** alongside *N*-BOC-DSA (**8**) and (+)-duocarmycin SA is illustrated in Figure 2, and the consensus alkylation selectivity is summarized in Table 1. Several important features are highlighted nicely in this figure. First and foremost, the simple derivatives are much less efficient (10^3−10^4 times) and exhibit a different and less selective DNA alkylation selectivity than duocarmycin SA. Like **8**, both enantiomers of **9** and **10** alkylate the same sites exhibiting an identical two base-pair AT-rich alkylation selectivity (5′-A<u>A</u> > 5′-T<u>A</u>), although there are subtle differences in the relative efficiencies of alkylation at the individual sites. The apparent preference of 5′-A<u>A</u> > 5′-T<u>A</u> is purely statistical, and the complementary unlabeled strand for the mixed sequence contains an identical 5′-TA site whose competitive alkylation diminishes the apparent alkylation efficiency of the labeled strand. Importantly, and different from conclusions reached in related studies,[5,12] we do not observe significant distinctions in the alkylation selectivities of such simple derivatives (BOC = $COCH_3$ = CO_2CH_3) and we find that they are all much less selective than **1**−**3**. The identical alkylation selectivity of both enantiomers of such simple derivatives is a natural consequence of the reversed binding orientations and the diastereomeric relationship of the adducts that result in the two enantiomers covering the exact same binding site surrounding the alkylated adenine. The factors controlling the alkylation selectivity are simply reaction at the sterically most accessible of the two most nucleophilic minor groove sites (adenine N3 versus guanine N3) and the depth of minor groove penetration available to the agent at the binding region surrounding the alkylation site. For the simple derivatives including **8**−**10**, this is possible only when the adjacent 5′ base is A or T. This has been discussed in detail elsewhere, and **9** and **10** conform nicely to the past observations.[6−10]

(19) Boger, D. L.; Coleman, R. S.; Invergo, B. J. *J. Org. Chem.* **1987**, *52*, 1521.

(20) Warpehoski, M. A.; Gebhard, I.; Kelly, R. C.; Krueger, W. C.; Li, L. H.; McGovren, J. P.; Prairie, M. D.; Wicnienski, N.; Wierenga, W. *J. Med. Chem.* **1988**, *31*, 590.

Table 1. Consensus Sequences for DNA Alkylation by Key Substructures and Analogs of Duocarmycin SA[a]

agent	base[b]	5′	4	3	2	1	0	−1	−2	−3	−4	3′
					Natural Enantiomers							
(+)-CC-1065	A/T (56)		67	78	94	98	100	55				
	consensus		A/T≥G/C	A/T>G/C	A/T	A/T	A	Pu≥Py				
(+)-DSA-CDPI$_2$	A/T (56)		71	85	100	100	100	63				
	consensus		A/T>G/C	A/T>G/C	A/T	A/T	A	Pu≥Py				
(+)-duocarmycin SA	A/T (56)			79	100	100	100	69				
	consensus			A/T>G/C	A/T	A/T	A	Pu>Py				
(+)-*N*-BOC-DSA	A/T (56)					95	100	65				
	consensus					A/T	A	Pu>Py				
					Unnatural Enantiomers							
(−)-*N*-BOC-DSA	A/T (56)					95	100	65				
	consensus					A/T	A	Pu≥Py				
(−)-duocarmycin SA	A/T (56)					93	100	96	73	56		
	consensus					A/T	A	A/T	A/T>G/C	N		
(−)-DSA-CDPI$_2$	A/T (56)					100	100	100	90	73	58	
	consensus					A/T	A	A/T	A/T>G/C	A/T>G/C	N	
(−)-CC-1065	A/T (56)					88	100	93	82	73	56	
	consensus					A/T	A	A/T	A/T>G/C	A/T>G/C	N	

[a] Percentage of the indicated base located at the designated position relative to the adenine-N3 alkylation site. [b] Percentage composition within the DNA examined.

The distinctions between the agents lie in the efficiencies of DNA alkylation. The natural enantiomers of **9** and **10** alkylate DNA at 10^{-3} M and were approximately 10 times more efficient than (+)-*N*-BOC-DSA. The similarities in **9** and **10** and the less effective DNA alkylation by *N*-BOC-DSA suggest that the differences simply may be due to the size of the substituent. The unnatural enantiomers of **9** and **10** were approximately 10 times less effective at alkylating DNA while the relative distinctions between (+)- and *ent*-(−)-*N*-BOC-DSA were smaller.[7] In addition to the much higher concentrations (10^3−10^4 times) required to detect alkylation with **8**−**10**, it also requires much more vigorous reaction conditions (37 °C, 24 h versus 4 °C, 2−10 h). In past studies, this has been attributed to the rate enhancement derived from the noncovalent minor groove binding of the full agents, positioning effects imposed on the DNA bound agents, or the relative degree of reversibility with such simple derivatives. While these effects contribute to the distinctions, we now suggest they fail to account for the full magnitude of the differences. In conjunction with our study of the agents described in the accompanying paper, we now suggest that in the absence of the extended right-hand subunit, DNA minor groove binding does not induce a twist in the N^2 amide and deprives the agent of this activation toward DNA alkylation.

Modifications in the Trimethoxyindole Subunit: Role of the Methoxy Substituents. DNA alkylation by the natural enantiomers of **22**−**25** were compared with that of **1** in w794 DNA (Supporting Information, Figure 1). All five agents exhibited identical DNA alkylation selectivities, and the distinctions observed were in the rates and efficiencies. When the incubation was conducted at 25 °C for 24 h, **23** was found to be essentially indistinguishable from **1** itself, **24** and **25** (**24** > **25**) were 5−10 times less efficient than **1**, and **22** was 20 times less efficient than **1** (Table 2). These trends in the efficiency of DNA alkylation were found to parallel the relative trends in cytotoxic potency. The relative rates of DNA alkylation for **1**, **23**, and **22** (10^{-5} M, 25 °C, 1−72 h) were also examined within w794 DNA at the single high affinity site of 5′-d(AATTA) (Supporting Information, Figure 2). (+)-Duocarmycin SA (**1**) and **23** were nearly indistinguishable with **1** exhibiting a slightly faster rate (k_{rel} = 1.3−2.3), and both were substantially faster than **22** (k_{rel} = 18−33).

Similar observations were made with the unnatural enantiomers (Table 2). Consistent with past observations, they all were found to alkylate DNA with a slower rate (*ca*. 50 times)[7] and lower efficiency (*ca*. 10 times) than the corresponding natural enantiomer. Detection of alkylation required both higher agent concentrations (10−50 times) and longer reaction times (72 versus 24 h) (Supporting Information, Figure 3). The distinctions between enantiomeric pairs of agents diminished as the number of methoxy groups was reduced and was greatest when the C5 methoxy group was present.

Table 2

agent	IC_{50} (pM, L1210)	rel DNA alkylation efficiency[a]	agent	IC_{50} (pM, L1210)	rel DNA alkylation efficiency[a]
	natural enantiomers			unnatural enantiomers	
(+)-**1**	10	1.0	(−)-**1**	100	0.1 (1.0)[a]
(+)-**23**	10−12	1.0	(−)-**23**	200	0.07 (0.7)
(+)-**24**	25	0.2	(−)-**24**	1300	0.04 (0.4)
(+)-**25**	60	0.1	(−)-**25**	1800	0.05 (0.5)
(+)-**22**	65	0.05	(−)-**22**	1700	0.03 (0.3)

[a] Within w794 DNA, 25 °C. The values in parenthesis are relative to *ent*-(−)-duocarmycin SA.

Thus, the C7 and C6 methoxy groups, which lie on the outer face of the DNA−agent complex, individually contribute little (C6 > C7) to the properties of duocarmycin SA. In contrast, the C5 methoxy group that is deeply imbedded in the minor groove contributes prominently to its properties. The agent containing a single C5 methoxy substituent proved essentially indistinguishable from duocarmycin SA, indicating that it alone is sufficient for observation of the full potency of the natural product. This is consistent with a role in which the C5 methoxy group provides further noncovalent binding stabilization for the inherently reversible DNA alkylation reaction[7,8,21] by virtue of its placement deep in the minor groove. More importantly, the C5 methoxy group of duocarmycin SA extends the rigid length of the DNA binding subunit (Figure 3). Its presence results in an increase in the inherent twist in the helical conformation of the DNA-bound agent with the helical rise of the agent adjusted at the site of linking amide.[15] This alters the vinylogous amide conjugation in the alkylation subunit and increases the inherent reactivity of the agent contributing to the catalysis of the DNA alkylation reaction. Removing the C5 methoxy substituent shortens the length of the right-hand subunit, decreases the

(21) Warpehoski, M. A.; Harper, D. H.; Mitchell, M. A.; Monroe, J. J. *Biochemistry* **1992**, *31*, 2502. Lee, C.-S.; Gibson, N. W. *Biochemistry* **1993**, *32*, 9108. Asai, A.; Nagamura, S.; Saito, H.; Takahashi, I.; Nakano, H. *Nucleic Acids Res.* **1994**, *22*, 88.

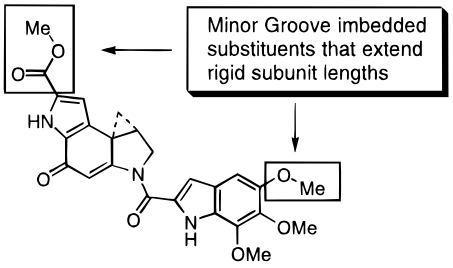

Figure 3.

inherent twist in the linking amide in the DNA bound conformation, and results in less effective activation of the agent for DNA alkylation.

Additional subtle features that were revealed include the unusual DNA alkylation efficiency of (+)-DSA-indole$_1$ (**22**). Although it proved to be 6−10 times less effective than duocarmycin SA, it is comparatively more effective than the indole derivative of CPI[20] or CBI.[7] Moreover, the relative DNA alkylation rates of the DSA-based agents substantially exceed those of the corresponding CPI-based agents despite their reduced reactivities.[7] We suggest this may be attributed to the presence of the C6 methyl ester which similarly extends the rigid length of the alkylation subunit. Consequently, even with a short suboptimal right-hand subunit, the presence of the C6 methyl ester insures more effective activation for DNA alkylation.

Extended Analogs: DSA-CDPI$_1$, DSA-CDPI$_2$, and DSA-indole$_2$. The examination of the agents **29**−**31** proved more important in studies than anticipated. Their side-by-side comparison with the reversed analogs detailed in the accompanying paper not only provided a definitive demonstration of the origin of the DNA alkylation selectivity but also provided insights into the source of catalysis. A comparison of the DNA alkylation by the natural enantiomers (+)-DSA-CDPI$_1$, (+)-DSA-CDPI$_2$, (+)-DSA-indole$_2$ alongside that of (+)-duocarmycin SA is shown in Figure 4. Under the conditions of the assay, **29**−**31** alkylated DNA at concentrations as low as 10^{-6}—10^{-7} M and did so with essentially the same efficiency. The consensus alkylation sequences for (+)- and *ent*-(−)-DSA-CDPI$_2$ are summarized in Table 1, and a table summarizing the statistical treatment of the alkylation sites that assesses the relative selectivity of (+)-DSA-CDPI$_2$ among the available alkylation sites may be found in the Supporting Information. Without exception, all alkylation sites proved to be adenine under the conditions of the assay. Each adenine alkylation site was flanked by at least two 5′ A or T bases with a preference that follows the order of 5′-AA<u>A</u> > 5′-TT<u>A</u> > 5′-TA<u>A</u> ≥ 5′-AT<u>A</u>. There was also a strong preference for the fourth and fifth 5′ bases to be A or T, and this preference distinguished the high-affinity versus low-affinity alkylation sites. Consistent with expectations, (+)- and *ent*-(−)-DSA-CDPI$_2$ exhibited a 5 base-pair AT-rich DNA alkylation selectivity identical to those of (+)- and *ent*-(−)-CC-1065 and distinguishable from the shorter 3.5 base-pair AT-rich selectivity of duocarmycin SA. Similar observations were made with (+)-DSA-indole$_2$. Consistent with observations first disclosed in efforts with (+)-CC-1065,[10] the relative selectivity of alkylation among the available sites proved to be greater with (+)-DSA-CDPI$_2$ than those with (+)-DSA-CDPI$_1$. Characteristic of this enhanced selectivity, (+)-DSA-CDPI$_2$ failed to alkylate the minor w794 site (5′-CAA<u>A</u>G) while (+)-DSA-CDPI$_1$ prominently alkylates this minor site, requiring concentrations only 10 times that for alkylation at the major 5′-AATT<u>A</u> site (Figure 4).

A comparison of the DNA alkylation by the unnatural enantiomers (−)-DSA-CDPI$_1$, (−)-DSA-CDPI$_2$, and (−)-DSA-indole$_2$ is provided (Supporting Information, Figure 4). Table 1 summarizes the DNA alkylation consensus sequence for *ent*-(−)-DSA-CDPI$_2$, and a statistical treatment assessing its relative selectivity among the available alkylation sites is summarized in the Supporting Information. The alkylation profiles of the unnatural enantiomers **29**−**31** are very distinct from those of the natural enantiomers. Without exception, all alkylation sites proved to be adenine under the conditions of the assay and nearly all of the 3′ and 5′ bases flanking the adenine N3 alkylation site proved to be A or T (Table 1). There proved to be a preference for the following three base-pair sequences: 5′-A<u>A</u>A > 5′-A<u>A</u>T ≥ 5′-T<u>A</u>A > 5′-T<u>A</u>T. Each high-affinity alkylation sites, *e.g.*, 5′-A<u>A</u>TTT, proved consistent with 5′ adenine alkylation with agent binding in the minor groove in the 5′ → 3′ direction from the alkylation site covering 3.5 or 5 base-pairs across an AT-rich region. The unnatural enantiomer AT-rich alkylation selectivity relative to the adenine N3 alkylation site is reversed and offset from that observed with the natural enantiomers. Consistent with expectations, *ent*-(−)-DSA-CDPI$_2$ exhibited a 5 base-pair AT-rich alkylation selectivity identical to *ent*-(−)-CC-1065 readily distinguishable from the shorter 3.5 base-pair selectivity of *ent*-(−)-duocarmycin SA and related smaller agents (Table 1). The unnatural enantiomers also exhibited a slower rate and lower efficiency (10−100 times) of DNA alkylation than the corresponding natural enantiomer.

Thus, the results suggest that the depth of minor groove penetration by the agent and steric accessibility to the alkylation

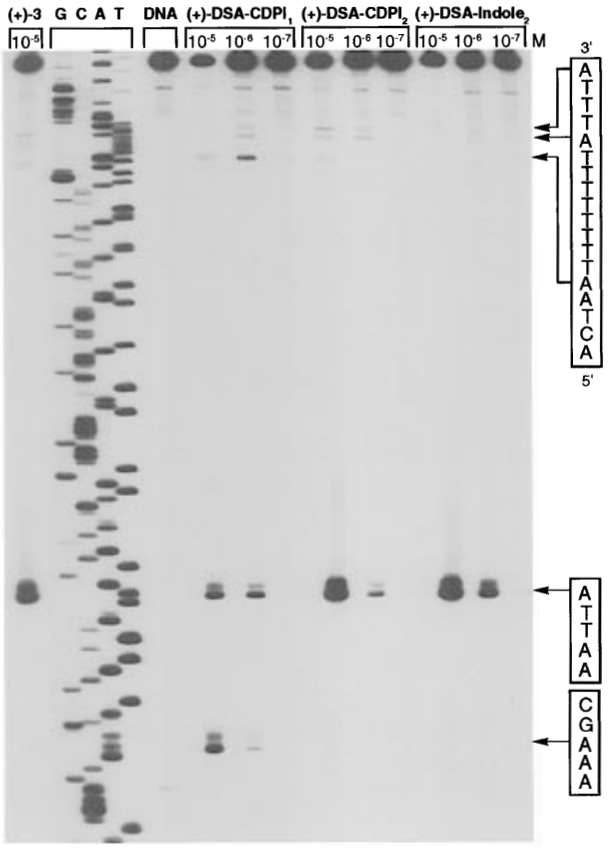

Figure 4. Thermally-induced strand cleavage of w794 DNA (144 bp, nucleotide no. 5238−138) after DNA−agent incubation at 25 °C (24 h), removal of unbound agent by EtOH precipitation, and 30 min of thermolysis (100 °C), followed by denaturing 8% PAGE and autoradiography. Lane 1, (+)-CC-1065 (1×10^{-5} M); lanes 2−5, Sanger, G, C, A, and T sequencing standards; lane 6, control DNA; lanes 7−9, (+)-DSA-CDPI$_1$ (1×10^{-5} to 1×10^{-7} M); lanes 10−12, (+)-DSA-CDPI$_2$ (1×10^{-5} to 1×10^{-7} M); lanes 13−15, (+)-DSA-indole$_2$ (1×10^{-5} to 1×10^{-7} M).

site are important features contributing to the observed selectivity of DNA alkylation. For simple derivatives of the alkylation subunit, sufficient minor groove access to the reacting center is possible with a single 5′ A or T base adjacent to the alkylation site. For the extended agents including **29**−**31**, sufficient minor groove penetration may be possible only when two or more adjacent bases are A or T, and this AT-rich selectivity nicely corresponds to the size of the agent (Table 1). Further contributing to this AT-rich alkylation selectivity of the longer agents is their preferential noncovalent binding within the narrower, deeper AT-rich groove.[22]

Rate of DNA Alkylation: pH Dependence. In our studies, we have qualitatively observed little pH dependence on the rate of DNA alkylation.[6−10] Moreover, in recent studies we have demonstrated that the rate of DNA alkylation for a series of closely related agents does not parallel the relative rates of acid-catalyzed nucleophilic addition to the activated cyclopropane.[7,23−25] Since these observations contrast with the proposed important role of acid catalysis for activation of the agents toward DNA alkylation[26] which has served as the basis for one prominent proposal for the origin of the DNA alkylation selectivity,[5,12,26,27] we elected to quantitate the effect of pH on the DNA alkylation rate. This was done by establishing the (+)-duocarmycin SA relative and first-order rate constants (k_{obsd}) for alkylation of the single w794 high-affinity alkylation site (5′-AATTA, see Figure 4) at pH values of 6.0, 6.6, 7.1, 7.6, and 8.1 (10^{-6} M, 25 °C, 10 mM phosphate buffer, 0−3 h). Because this was conducted using w794 DNA additionally containing >7000 base-pairs and multiple binding sites within the unlabeled portion of the DNA, the comparisons were conducted at concentrations that provide saturated binding and restrict the kinetic analysis to the pseudo-first-order rate constant for alkylation. Although the rate of DNA alkylation was found to increase with decreasing pH, the rate change was small (<2 times over 2 pH units) and inconsistent with a first-order dependence on acid concentration (Figure 5). Moreover, between pH 7 and 8, which may be considered the most relevant range, the rate dependence on pH essentially disappeared. Just as significant, comparison of the psuedo-first-order rate constant for DNA alkylation at this site, $k = 1.69 \times 10^{-4}$ s^{-1} (pH 7.1), with the calculated pseudo-first-order rate constant for acid-catalyzed solvolysis ($k = 1.08 \times 10^{-10}$ s^{-1}) at pH 7 revealed that the bulk of catalysis for the DNA alkylation reaction cannot be accounted for by this source. Perhaps the magnitude of this difference is best recognized by simply stating that at pH 7, the $t_{1/2}$ for solvolysis is 202 years (7.4×10^4 days) while that of DNA alkylation is 1.1 h. The relative lack of dependence on the acid concentration (pH) especially in the most relevant pH range of 7−8 in conjunction with the observations made in the accompanying paper has led us to propose an alternative source of reaction catalysis.[15]

pH	k (s^{-1})	k_{rel}
6.0	2.83×10^{-4}	1.89
6.6	1.99×10^{-4}	1.32
7.1	1.69×10^{-4}	1.12
7.6	1.58×10^{-4}	1.05
8.1	1.50×10^{-4}	1.0

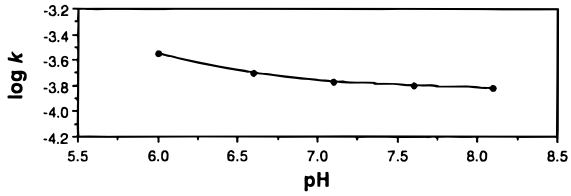

Figure 5. Tabulation of DNA alkylation rate pH dependence and plot of log k_{obsd} versus pH for the (+)-duocarmycin SA (1×10^{-6} M) alkylation at the w794 DNA high affinity site, 5′-d(AATTA)-3′.

Catalysis: DNA Binding-Induced Conformational Change in the Agent Results in Activation. In conjunction with the studies disclosed in the accompanying paper which document both the extent and structural origin of the rate acceleration for the DNA alkylation reaction, an alternative source of catalysis became apparent. These studies along with a number of additional unrelated observations have led us to propose that catalysis for the DNA alkylation reaction is derived from a DNA binding-induced conformational change in the agent that disrupts the vinylogous amide stabilization of the alkylation subunit and activates the agent for nucleophilic addition.[15] This conformational change results from adoption of a helical-bound conformation that follows the curvature and pitch of the DNA minor groove. The helical rise in the bound conformation of the rigid agents is adjusted by twisting the linking N^2 amide, which is the only available flexible site. The twisting of the χ_1 dihedral angle of the linking amide ($\chi_2 \approx 0°$) diminishes the N^2 lone pair conjugation with the cyclohexadienone, disrupts the vinylogous amide stabilization of the alkylation subunit, and increases its inherent reactivity (Figure 6). An alternative possibility involves a twisting of the χ_2 dihedral angle diminishing the amide conjugation and increasing the N^2 vinylogous amide conjugation. This would increase the basicity of the C4 carbonyl leading to more effective protonation. There is evidence to suggest this can result in both increased[28] or decreased reactivity[15] (Figure 6) depending on the extent of the vinylogous amide conjugation, and all studies concur that even subtle perturbations can result in large changes in reactivity. While our present studies do not distinguish between these two possibilities, the former reflects the changes observed in going to the product of the reaction (fully engaged amide, $\chi_2 = 0°$; no vinylogous amide, $\chi_1 \approx 20-35°$ and lengthened bond c).[15] It is consistent with a DNA bound conformation of duocarmycin SA established by ^{1}H NMR which exhibited at $44 \pm 2°$ twist between the planes of the two subunits with the bulk of the twist being accommodated in χ_1.[15] In addition, we have observed remarkably large and appropriate reactivity changes that accompany such a decoupling of the vinylogous amide including that resulting from a twist in the χ_1 dihedral angle which is consistent with this as a source of catalysis (Figure 6).

N-Acylation of the nitrogen (*e.g.*, *N*-CO_2Me-CNA versus CNA) reduces the vinylogous amide conjugation, lengthens bond c, and results in a substantial increase in inherent reactivity. Typically accompanying this reduction in the vinylogous amide conjugation is an increase in the length of the reacting

(22) Boger, D. L.; Coleman, R. S.; Invergo, B. J.; Zarrinmayeh, H.; Kitos, P. A.; Thompson, S. C.; Leong, T.; McLaughlin, L. W. *Chem. Biol. Interact.* **1990**, *73*, 29. Boger, D. L.; Zhou, J.; Cai, H. *Bioorg. Med. Chem.* **1996**, *4*, 859.

(23) Boger, D. L.; Han, N.; Tarby, C. M.; Boyce, C. W.; Cai, H.; Jing, Q.; Kitos, P. A. *J. Org. Chem.* **1996**, *61*, 4894. Boger, D. L.; McKie, J. A.; Cai, H.; Cacciari, B.; Baraldi, P. G. *J. Org. Chem.* **1996**, *61*, 1710.

(24) Boger, D. L.; Boyce, C. W.; Johnson, D. S. *Bioorg. Med. Chem. Lett.* **1997**, *7*, 233.

(25) Boger, D. L.; Munk, S. A.; Ishizaki, T. *J. Am. Chem. Soc.* **1991**, *113*, 2779. Boger, D. L.; Munk, S. A. *J. Am. Chem. Soc.* **1992**, *114*, 5487.

(26) Warpehoski, M. A.; Harper, D. E. *J. Am. Chem. Soc.* **1994**, *116*, 7573. Warpehoski, M. A.; Harper, D. E. *J. Am. Chem. Soc.* **1995**, *117*, 2951.

(27) Warpehoski, M. A.; McGovren, P.; Mitchell, M. A. In *Molecular Basis of Specificity in Nucleic Acid-Drug Interactions*; Pullman, B., Jortner, J., Eds.; Kluwer: Dordrecht, The Netherlands, 1990; p 531.

(28) Boger, D. L.; Yun, W. *J. Am. Chem. Soc.* **1994**, *116*, 5523.

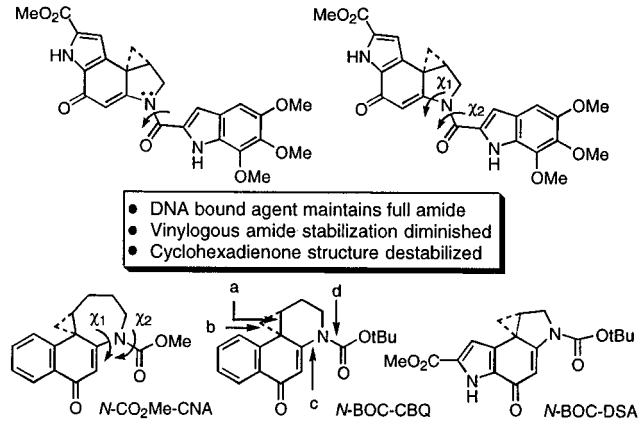

X-ray bond lengths, Å	*N*-CO_2Me-CNA	*N*-BOC-CBQ[29]	*N*-BOC-DSA
a	1.565	1.528	1.519
b	1.525	1.543	1.550
c	1.428	1.415	1.393
d	1.357	1.379	1.375
X-ray dihedral angles			
χ_1	86.4°	34.2°	6.9°
χ_2	3.9°	8.7°	4.5°
solvolysis reactivity			
k, s^{-1} (pH 3)	6.78×10^{-3}	9.07×10^{-5}	1.08×10^{-6}
$t_{1/2}$, (pH 3)	0.028 h	2.1 h	177 h
k, s^{-1} (pH 7)	9.16×10^{-5}	3.54×10^{-7}	stable
$t_{1/2}$, (pH 7)	2.1 h	544 h	stable

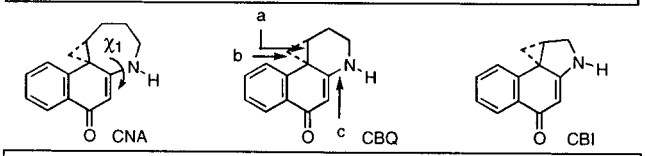

X-ray bond lengths, Å	CNA	CBQ	CBI[18]
a	1.543	1.525	1.508
b	1.551	1.539	1.532
c	1.376	1.336	1.337
X-ray dihedral angle[a]			
χ_1	50.7°	6.9°	11.4°
solvolysis reactivity			
k, s^{-1} (pH 3)	3.10×10^{-4}	2.11×10^{-6}	2.07×10^{-7}
$t_{1/2}$, (pH 3)	0.62 h	91 h	930 h

[a]Calculated assuming sp^2 nitrogen

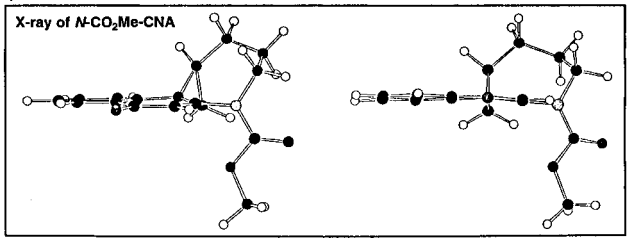

Figure 6.

cyclopropane bond. One interpretation of this is that both the cyclopropane conjugation and its inherent reactivity increase as the cross-conjugated vinylogous amide π-overlap is diminished. Additional features including the alignment of the cyclopropane may further contribute to the cyclopropane conjugation (CBQ aligned but CBI offset by 20°), and the cyclopropane bond lengths and reactivity of CBQ versus CBI also reflect this effect on the relative degree of conjugation. This has been discussed in detail elsewhere.[29] More importantly, within the series of *N*-acyl derivatives illustrated in Figure 6, both the length of bond c diagnostic of the extent of vinylogous amide conjugation and the reactivity smoothly increase as the χ_1 dihedral angle increases. The reactivity of *N*-CO_2Me-CNA (or *N*-BOC-CNA) is extraordinary, exhibiting a $t_{1/2}$ of only 2.1 h at pH 7 in the absence of deliberate added acid catalysis. It is 10^3-10^4 times more reactive than *N*-BOC-DSA and represents an agent that benefits from little, if any, vinylogous amide stabilization. This level of reactivity is greater than that required. In fact, it is the reactivity and χ_1 dihedral angle of *N*-BOC-CBQ that may more closely approximate that required for the DNA alkylation catalysis provided by the DNA binding-induced conformational change in **1**−**3**. Its inherent reactivity at pH 7 coupled with the rate enhancements afforded a bound species that might provide a further 10^2 times rate acceleration approximates the rates observed with the DNA alkylation reaction.

This has important ramifications on the source of the DNA alkylation selectivity. The inherent twist and helical rise of the bound conformation of the agent is greatest within the narrower, deeper AT-rich minor groove. This leads to preferential activation of the agent for DNA alkylation within extended AT-rich minor groove sites and complements their preferential AT-rich noncovalent binding selectivity.[22] Thus, both shape-selective recognition (preferential AT-rich noncovalent binding) and shape-dependent catalysis (extended AT-rich > GC-rich activation by twist in N^2 amide) combine to restrict S_N2 alkylation to accessible adenine N3 nucleophilic sites within the preferred binding sites. Importantly, this ground state destabilization of the substrate only activates the agent (*e.g.*, arms the warhead) for a rate-determining S_N2 nucleophilic addition and requires the subsequent proper positioning and accessibility to an adenine N3 site. Although a subtle point, this accounts nicely for the identical alkylation selectivities of CC-1065 (**1**) and **32**−**34**[30] which lack both the C4 carbonyl and the activated cyclopropane but which alkylate DNA at substantially slower rates. Thus, the alkylation selectivity is controlled by the identical AT-rich noncovalent binding selectivity of the agents, but **32**−**34** react much slower in part because they lack the capabilities for activation by the DNA binding-induced conformation change.

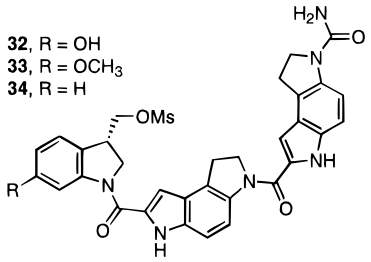

This source of catalysis requires an extended and rigid N^2 amide substituent,[16] and the absence of such a substituent with **8**-**10** accounts nicely for their relatively slow and ineffective DNA alkylation. As detailed in the accompanying paper, the noncovalent binding derived from the attached right-hand subunits accounts for a much smaller part of the difference in the rates of DNA alkylation between **8**−**10** and **1**. More importantly, this source of catalysis would lead to distinctions, not similarities, in the DNA alkylation selectivities of **8**−**10** versus **1** contrary to the consequences of alternative proposals that have been advanced in related studies.[5,12,31]

Reaction Regioselectivity and Stereochemistry: Subtle Features Contributing to the DNA Alkylation Regioselec-

(29) Boger, D. L.; Mésini, P. *J. Am. Chem. Soc.* **1994**, *116*, 11335. Boger, D. L.; Mésini, P. *J. Am. Chem. Soc.* **1995**, *117*, 11647.

(30) Boger, D. L.; Munk, S. A.; Zarrinmayeh, H. *J. Am. Chem. Soc.* **1991**, *113*, 3980.

Scheme 5

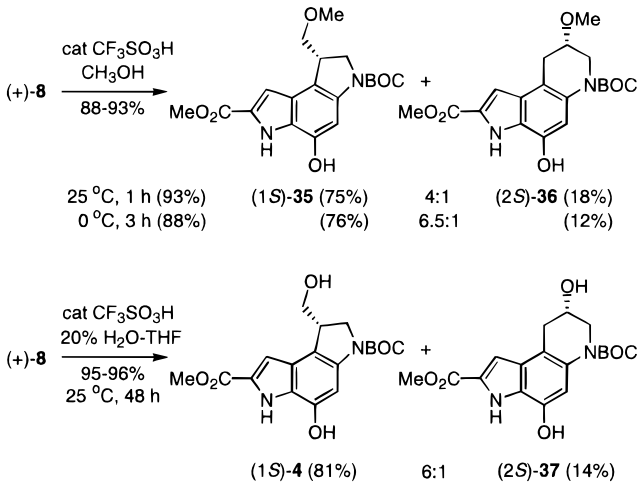

tivity. Studies of the inherent solvolysis regioselectivity and stereochemistry in conjunction with the structural studies have also provided important insights into the mechanism of nucleophilic addition and subtle features contributing to the regioselectivity of the DNA alkylation reaction. A study of the acid-catalyzed nucleophilic additions to *N*-BOC-DSA (**8**) established that solvolysis preferentially occurs with cleavage of the C7b−C8 bond with addition of a nucleophile to the least-substituted C8 cyclopropane carbon versus cleavage of the C7b−C8a bond with ring expansion and addition to C8a. The latter cleavage would place a developing partial positive charge on a preferred secondary versus primary center, and this preference was overridden by the inherent stereoelectronic control of the reaction regioselectivity. Preparative acid-catalyzed addition of CH_3OH to *N*-BOC-DSA (0.12 equiv of CF_3SO_3H, 0.01 M in CH_3OH, 0 or 25 °C, 1−3 h, 88−93%) cleanly provided two products **35** and **36** in a 6.5−4:1 ratio with the greater selectivity observed at 0 versus 25 °C (Scheme 5). Similarly, solvolysis of **8** (0.24 equiv of CF_3SO_3H, 0.01 M in 20% H_2O/THF, 25 °C, 48 h, 95−96%) provided a 6:1 ratio of **4** to **37**. The mechanistic course of the reaction was established by subjecting both racemic and natural (+)-**8** to the acid-catalyzed methanolysis or solvolysis. Resolution on a Diacel ChiralCel AD HPLC column separated both enantiomers of the two reaction products, and those derived from optically active (+)-**8** were found to consist of a single enantiomer. Although the generation of a single enantiomer of **35** would be consistent with either a S_N1 or S_N2 ring-opening reaction, the generation of a single enantiomer of **36** establishes that the ring expansion proceeds with clean inversion of the reaction center stereochemistry in a S_N2 reaction. This is consistent with kinetic studies of the acid-catalyzed nucleophilic addition where the rate of reaction exhibits a first-order dependence on both the acid concentration (pH) as well as the nucleophile indicative of a mechanism involving rapid and reversible C4 carbonyl protonation followed by a slow, rate-determining S_N2 nucleophilic attack on the activated cyclopropane.

Important insights into the solvolysis regioselectivity may be derived from the structural studies conducted to date (Figure 7). The distinguishing feature controlling the regioselectivity appears to be the relative stereoelectronic alignment of the two

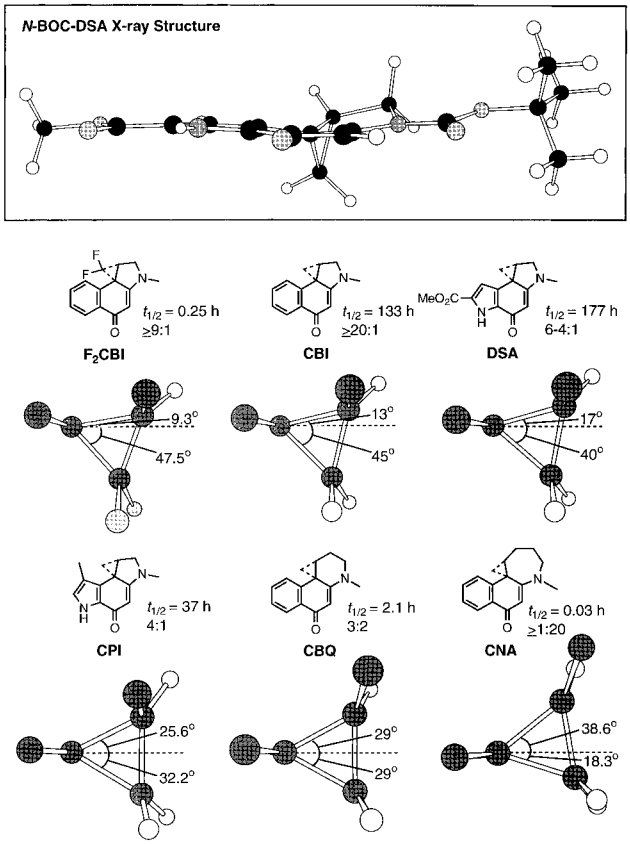

Figure 7. Models of the side views of the activated cyclopropanes of six X-ray crystal structures highlighting the relative stereoelectronic alignment of the cyclopropane bonds. Solvolysis half-life (pH 3) and regioselectivity of the *N*-BOC derivatives are given.

cyclopropane bonds available for cleavage. Within a class of agents whose cyclopropane alignment with the π-system would be expected to be similar due to structural constraints, the regioselectivity nicely follows the reactivity with the more stable agents providing the more selective reaction, *e.g.*, *N*-BOC-DSA (6−4:1) > CPI (4:1) > *N*-BOC-DA (3:2). However, this fails to hold true when comparing between classes of agents, *e.g.*, *N*-BOC-CBI (≥20:1) versus *N*-BOC-DSA (6−4:1) versus *N*-BOC-CNA (≤1:20). Thus, additional important factors contribute to this reaction regioselectivity. In the comparisons that can be made from the available X-ray structures, the selectivity more accurately reflects the relative degree of stereoelectronic alignment of the two available cyclopropane bonds, and this alone accounts for the reaction regioselectivity (Figure 7). This is illustrated beautifully with the observation of the clean, smooth, and complete reversal of the reaction regioselectively as one progress through the series *N*-BOC-CBI (≥20:1), *N*-BOC-CBQ (3:2), and *N*-BOC-CNA (≤1:20).

The observation of exclusive adenine N3 addition to the C8 cyclopropane carbon in the DNA alkylation studies of **1** and related agents is not consistent with expectations that the inherent acid-catalyzed nucleophilic addition regioselectivity controls the DNA alkylation regioselectivity. This exclusive DNA alkylation regioselectivity was not only observed in our studies with **1** or **2** and their enantiomers but is general with all agents examined to date that undergo solvolysis with a mixed regioselectivity including the CPI-based agents and CC-1065 (4:1 regioselectivity) and the CBQ-based agents (3:2 regioselectivity). Examination of each of these agents has led only to detection of adducts derived from adenine N3 addition to the least-substituted cyclopropane carbon. Moreover, each of these studies quantitated the adduct formation and, for duocarmycin

(31) Lin, C. H.; Sun, D.; Hurley, L. H. *Chem. Res. Toxicol.* **1991**, *4*, 21. Lee, C.-S.; Sun, D.; Kizu, R.; Hurley, L. H. *Chem. Res. Toxicol.* **1991**, *4*, 203. Lin, C. H.; Hill, G. C.; Hurley, L. H. *Chem. Res. Toxicol.* **1992**, *5*, 167. Ding, Z.-M.; Harshey, R. M.; Hurley, L. H. *Nucleic Acids Res.* **1993**, *21*, 4281. Sun, D.; Lin, C. H.; Hurley, L. H. *Biochemistry*, **1993**, *32*, 4487. Thompson, A. S.; Sun, D.; Hurley, L. H. *J. Am. Chem. Soc.* **1995**, *117*, 2371.

A (86−92%),[9] duocarmycin SA (95−100%),[7] CC-1065 (> 85%),[12] and the CBQ-based agents (>75%),[29] established that the regioselectivity of the DNA alkylation reaction is greater than that of solvolysis. Although several explanations may be advanced for these observations,[29] the three most prominent are (1) preferential adoption of binding orientations that favor normal adenine N3 addition (proximity effects), (2) the adoption of DNA bound conformations that impose full stereoelectronic control on the reaction, and (3) the significant destabilizing torsional strain and steric interactions that accompany the abnormal addition. Figures illustrating these effects have been disclosed in our work,[29] and we would suggest that the latter subtle effect of preferential S_N2 addition of a large nucleophile to the least-substituted carbon is most substantial. Consequently, the clean regioselectivity of the characteristic adenine N3 alkylation reaction benefits not only from stereoelectronic control but additional important subtle effects characteristic of the S_N2 addition of a large nucleophile that further enhance the normally observed regioselectivity.

Reversibility. The cyclopropane ring of the duocarmycins is very easily introduced through Ar−3′ spirocyclization (*cf*., Schemes 2−4). This occurs so readily that the precursor agents will often close upon formation or upon exposure to chromatography supports (*e.g*., SiO_2). Although the reactions are usually conducted with strong base (NaH, 1,8-diazabicyclo-[5.4.0]undec-7-ene (DBU), Et_3N), the most stable of the agents including **4** may be prepared by simple exposure to even aqueous 2−5% $NaHCO_3$. In early studies, this suggested to us that the adenine N3 adduct in DNA should be formed in a readily reversible manner.[6−10,32] Ultimately, this proved to be the case, although the degree of reversibility was lower and the rate of retroalkylation was slower than the chemical precedent would suggest.[7,8,21] The unusual stability of the DNA adducts and the slow rate of retroalkylation has been attributed to the noncovalent binding stabilization provided by the right-hand subunits.[6,15] We now suggest that the adoption of the DNA bound and alkylated conformation no longer facilitates Ar-3′ spirocyclization with reversal of the DNA alkylation reaction and that this further contributes to the unusual stability of the DNA adducts. Not only does this ground state destabilization of the substrate account for the rate acceleration for formation of adduct by lowering the apparent activation energy but it contributes to a shift in the equilibrium to favor adduct formation since the product does not contain the vinylogous amide and is not similarly destabilized by adopting a helical conformation.[15] This subtle feature, in our assessment, may be more important to the expression of the biological properties than even the role in catalysis.

Conclusions. Of the naturally occurring agents, duocarmycin SA is chemically the most stable and biologically the most potent. It exhibits the greatest inherent reaction regioselectivity and participates most effectively in the characteristic DNA alkylation reaction. The comparison of six X-ray structures suggests that the relative degree of stereoelectronic alignment of the two available cyclopropane bonds alone may account for the solvolysis regioselectivity. The exclusive DNA alkylation regioselectivity of the adenine N3 addition reaction exceeds that of the typical acid-catalyzed reactions for all agents examined to date. Several explanations may account for the observations including the adoption of binding orientations that favor the normal addition, the adoption of DNA-bound conformations that impose complete stereoelectronic control on the reaction, and the destabilizing torsional strain and steric interactions that accompany the abnormal addition. We suggest the latter effects are most significant and simply represent the expected preferential S_N2 addition of a large, hindered nucleophile to the least substituted secondary versus tertiary carbon of the activated cyclopropane.

The DNA alkylation selectivity of both enantiomers of a series of analogs of **1** was examined and proved consistent with prior studies. Both enantiomers of simple derivatives of the alkylation subunit (**8**−**10**) behave comparably and alkylate the same sites in DNA (5′-A<u>A</u> > 5′-T<u>A</u>). This unusual behavior of the enantiomeric agents is a natural consequence of the reversed binding orientations, and the diastereomeric relationship of the adducts that result in the two enantiomers covering the exact same binding site surrounding the alkylated adenine. The advanced analogs of **1**−**3** exhibited a different and larger 3.5 or 5 base-pair AT-rich adenine N3 alkylation selectivity that corresponds nicely to the length or size of the agent. For the natural enantiomers, the alkylation sites correspond to 3′ adenine N3 alkylation with agent binding in the 3′ → 5′ direction across a 3.5 or 5 base-pair AT-rich sequence, *e.g*., 5′-AAAA<u>A</u>. For the unnatural enantiomers, the alkylation sites correspond to 5′ adenine N3 alkylation with agent binding in the reverse 5′ → 3′ direction across a 3.5 or 5 base-pair AT-rich sequence that starts with the 5′ base that precedes the alkylated adenine and extends over the alkylation site to the adjacent 3′ side, *e.g*., 5′-A<u>A</u>AAA.

A study of the pH dependence of the rate of DNA alkylation revealed little effect in the pH range of 7−8 and only a modest effect below pH 7. This proved consistent with recent observations that the rate of DNA alkylation does not necessarily follow the relative rates of acid-catalyzed nucleophilic addition.[7,23−25] As a consequence of this and consistent with the emerging model of the origin of the DNA alkylation selectivity, an alternative mechanism of activating the agent for DNA alkylation was introduced on the basis of a DNA binding-induced conformational change in the agent which twists the linking N^2 amide and disrupts the vinylogous amide stabilization of the alkylation subunit. Further support of this mechanism of activation is provided in the accompanying paper. An important consequence of this source of activation is that it is expected to be greatest within the narrower, deeper AT-rich minor groove further complementing the noncovalent minor groove binding selectivity of the agents. Thus, the shape-selective binding selectivity and shape-dependent catalysis combine to restrict S_N2 alkylation to accessible adenine N3 nucleophilic sites within the preferred 3.5−5 base-pair AT-rich binding sites.

The study of analogs containing modifications in the trimethoxyindole subunit revealed that the C5 methoxy substituent is necessary and sufficient for observation of the full effectiveness of the natural product while the C6 and C7 (C6 > C7) methoxy substituents contribute little to its properties. In addition to its contribution to the noncovalent binding stabilization derived from its imbedded minor groove location, its simple presence increases the rigid length of the right-hand subunit increasing the inherent twist in the DNA-bound helical conformation. This more effectively disrupts the vinylogous amide stabilization in the alkylation subunit and further increases the inherent reactivity of the DNA bound agent. A similar role is proposed for the C6 methyl ester which extends the rigid length of the left-hand alkylation subunit.

The agents exhibited cytotoxic potencies consistent with the trends observed in the relative DNA alkylation efficiencies and each of the analog classes was found to follow a well-established relationship between chemical stability and cytotoxic potency. Since the duocarmycin SA alkylation subunit is the most stable of the naturally occurring alkylation subunits, its derivative

(32) Boger, D. L.; Coleman, R. S. *J. Am. Chem. Soc.* **1988**, *110*, 4796.

analogs are the most potent disclosed to date. These studies are summarized in the following paper.

Experimental Section

Resolution of *N*-BOC-DSA (8). 2-Propanol and hexane (Fisher, HPLC grade) were filtered through a Millipore HV filter (pore size = 0.45 μm) and degassed by stirring under vacuum. A Waters Prep LC 4000 HPLC system equipped with a Diacel ChiralCel OD column (2 × 25 cm, 10 μm) was equilibrated with 30% 2-propanol/hexane at a flow rate of 7 mL/min. (±)-*N*-BOC-DSA (**8**)[17] was dissolved in CH_3OH (20 mg/mL), and 0.5−1.0 mL (10−20 mg) aliquots were injected at 20−25 min intervals. The effluent was monitored at 254 nm, and the fractions containing resolved **9** were collected: natural (+)-**8** (t_R = 19.5 min) and *ent*-(−)-**8** (t_R = 23.5 min), α = 1.24.

General Procedure for the Preparation of 18−21 and 26−28. Methyl 3-[[5-[((1*H*-Indol-2-yl)carbonyl)amino]-1*H*-indol-2-yl]carbonyl]-1-(chloromethyl)-5-hydroxy-1,2-dihydro-3*H*-pyrrolo[3,2-*e*]indole-7-carboxylate (28). A solution of **5**[17] (2.0 mg, 5.25 μmol) in 4 N HCl/EtOAc (0.25 mL) was stirred for 20 min at 25 °C. The reaction mixture was concentrated to afford **7** as a gray powder. The hydrochloride salt was taken up in DMF (0.12 mL) and treated sequentially with 1-(3-(dimethylamino)propyl)-3-ethylcarbodiimide hydrochloride (EDCI, 3.5 mg, 15.75 μmol, 3.3 equiv) and indole$_2$ (1.9 mg, 6.04 μmol, 1.1 equiv). The reaction mixture was stirred for 12 h at 25 °C before the solvent was removed under reduced pressure. The residual solid was slurried in 0.1 mL of H_2O, and the solid was collected by centrifugation. Chromatography (1 × 5 cm SiO_2, 20% DMF/toluene) afforded **28** (2.5 mg, 81%) as a gray solid: mp > 230 °C; ^{1}H NMR (DMSO-d_6, 400 MHz) δ 11.73 (d, 1H, J = 1.2 Hz, NH), 11.68 (d, 1H, J = 1.6 Hz, NH), 11.65 (s, 1H, NH), 10.61 (s, 1H, NH), 9.83 (s, 1H, OH), 8.20 (d, 1H, J = 1.6 Hz), 7.82 (br s, 1H), 7.67 (d, 1H, J = 7.9 Hz), 7.55 (dd, 1H, J = 8.8, 1.8 Hz), 7.48 (s, 1H), 7.46 (s, 1H), 7.42 (s, 1H), 7.29 (1H, J = 2.0 Hz), 7.21 (dt, 1H, J = 8.2, 1.2 Hz), 7.15 (d, 1H, J = 1.4 Hz), 7.06 (dt, 1H, J = 8.0, 0.8 Hz), 4.77 (t, 1H, J = 10.6 Hz, C2-H), 4.45 (dd, 1H, J = 10.9, 3.9 Hz, C2-H), 4.15−4.05 (m, 2H), 3.98 (dd, 1H, J = 7.0, 3.9 Hz), 3.87 (s, 3H, OCH_3); IR (neat) ν_{max} 3393, 2966, 2916, 1711, 1693, 1662, 1646, 1631, 1612, 1553, 1537, 1517, 1485, 1234, 1134 cm^{-1}; FAB HRMS (NBA/NaI) *m/z* 582.1540 (M^+ + H, $C_{31}H_{24}N_5O_5Cl$ requires 582.1544).

1(*S*)-**28**: $[\alpha]^{23}_D$ +27° (*c* 0.15, DMF).

ent-1(*R*)-**28**: $[\alpha]^{23}_D$ −29° (*c* 0.10, DMF).

General Procedure for the Preparation of 22−25 and 29−31. Methyl 2-[[5-[((1*H*-Indol-2-yl)carbonyl)amino]-1*H*-indol-2-yl]carbonyl]-4-oxo-1,2,8,8a-tetrahydrocyclopropa[*c*]pyrrolo[3,2-*e*]indole-6-carboxylate (31, DSA-indole$_2$). A portion of NaH (0.4 mg, 60%, 10.3 μmol, 3 equiv) at 0 °C under Ar was treated with a solution of **28** (2.0 mg, 3.4 μmol, 1.0 equiv) in DMF (0.25 mL), and the reaction mixture was stirred for 90 min at 0 °C. The reaction mixture was directly subjected to flash chromatography (1 × 5 cm SiO_2, 15% DMF/toluene) to afford **31** (1.6 mg, 85%) as a pale yellow solid: mp > 230 °C; ^{1}H NMR (DMSO-d_6, 400 MHz) δ 12.64 (s, 1H, NH), 11.81 (d, 1H, J = 1.6 Hz, NH), 11.72 (d, 1H, J = 1.2 Hz, NH), 10.18 (s, 1H, OH), 8.20 (d, 1H, J = 1.5 Hz), 7.66 (d, 1H, J = 8.0 Hz), 7.59 (dd, 1H, J = 8.9, 2.0 Hz), 7.47 (s, 1H), 7.45 (s, 1H), 7.41 (d, 1H, J = 1.4 Hz), 7.22 (d, 1H, J = 2.2 Hz), 7.20 (dd, 1H, J = 8.2, 1.1 Hz), 7.06 (dt, 1H, J = 7.5, 0.7 Hz), 6.80 (s, 1H), 6.79 (d, 1H, J = 7.1 Hz), 4.58 (dd, 1H, J = 10.5, 5.1 Hz, C1-H), 4.44 (d, 1H, J = 10.5 Hz, C1-H), 3.79 (s, 3H, OCH_3), 3.05 (m, 1H, C8a-H), 1.78 (dd, 1H, J = 7.7, 3.8 Hz, C8-H), 1.60 (t, 1H, J = 4.5 Hz, C8-H); IR (neat) ν_{max} 3317, 2953, 2921, 2853, 1712, 1658, 1649, 1642, 1592, 1554, 1515, 1390, 1310, 1260 cm^{-1}; FAB HRMS (NBA) *m/z* 546.1789 (M^+ + H, $C_{31}H_{23}N_5O_5$ requires 546.1777).

(+)-**31**: $[\alpha]^{23}_D$ +65° (*c* 0.16, DMF).

ent-(−)-**31**: $[\alpha]^{23}_D$ −69° (*c* 0.19, DMF).

Acknowledgment. We gratefully acknowledge the financial support of the National Institutes of Health (CA55276), the Skaggs Institute for Chemical Biology, and the award of predoctoral (D.S.J., ACS Organic Division sponsored by Zeneca Pharmaceuticals, 1993−94; Eli Lilly, 1995−1996; J.G., NDSEG-1995) and postdoctoral fellowships (D.L.H., NIH CA09303; B.B., Deutsch Fellowship Bo-1309/1-1).

Supporting Information Available: Summary tables of the comparison cytotoxicity testing data, experimental procedures and characterization of **9**−**12**, **18**−**27**, **29**, and **30**, experimental procedures for the solvolysis studies of (+)- and (±)-**8** and the DNA alkylation studies, tables of the statistical treatment of the sites of DNA alkylation by (+)-and *ent*-(−)-DSA-CDPI$_2$, gel figures of (+)-**22**−**25** (Figure 1), *ent*-(−)-**22**−**25** (Figure 3), and *ent*-(−)-**29**-**31** (Figure 4), a figure of the DNA alkylation rate comparison of (+)-**1**, (+)-**22**, and (+)-**23** (Figure 2), and details of the X-ray structures of *N*-CO_2Me-CNA, *N*-BOC-DSA, CNA, *seco*-*N*-BOC-CNA, and CBQ not previously disclosed (102 pages). See any current masthead page for ordering and Internet access instructions.

JA9637208